Available online at www.sciencedirect.com
ScienceDirect
Journal of the Chinese Institute of Chemical Engineers 39 (2008) 75–83
JOURNAL OF THE CHINESE INSTITUTE OF CHEMICAL ENGINEERS
www.elsevier.com/locate/jcice

An observation of the coexistence of multimers and micelles in a nonionic surfactant $C_{10}E_4$ solution by dynamic light scattering

Ya-Chi Lee [a], Hwai-Shen Liu [b], Shi-Yow Lin [a,*], Hsiu-Fen Huang [a], Yung-Yu Wang [a], Li-Wei Chou [a]

[a] *Department of Chemical Engineering, National Taiwan University of Science and Technology, Taipei 106, Taiwan*
[b] *Department of Chemical Engineering, National Taiwan University, Taipei 106, Taiwan*

Received 23 August 2007; accepted 20 November 2007

Abstract

The bulk phase of nonionic surfactant $C_{10}E_4$ solution was monitored by a dynamic light scattering (DLS) system at 20 °C in a narrow range of concentration near the cmc. Two particle aggregations were observed. The DLS data show (i) there exist premicellar multimers (or called sub-micelles) and (ii) micelles coexist with multimers. The $C_{10}E_4$ sub-micelles have a narrow size distribution with an averaged hydrodynamic diameter (D_h) of 1.35 nm. The D_h of the micelles is around 10.5 nm at 1.0×10^{-6} mol/mL and increases slightly with $C_{10}E_4$ concentration. It is illustrated from the DLS data that (i) at $C = 0.78$–0.82 μmol/mL, monomers and premicellar multimers coexist and (ii) at $C = 0.84$–0.92 μmol/mL, monomers + submicellar multimers + micelles coexist. At more elevated concentrations, only the signals from the micelles are detected by DLS.

Keywords: Dynamic light scattering; Micelles; Multimers; Pre-micelles; Sub-micelles; Surfactant

1. Introduction

Pre-micelles are low-molecular weight aggregates or clusters that consist of a few or several surfactant molecules in surfactant solutions. Micelles and pre-micelles have attracted much attention because of their enormous potential for practical applications as well as their interesting physical properties. Formation of pre-micelles has been proposed due to the observations of some specific property changes in surfactant solutions below or around the critical micelle concentration (cmc).

A catalytic effect (Cho and Morawetz, 1972; Pérez-Benito and Rodenas, 1990; Uppu, 1995) and an enhancement of reaction rate (Bruhn and Holzwarth, 1978; Holzwarth *et al.*, 1978) have been reported for surfactant solutions below cmc. A water solubility enhancement of insoluble compounds was observed in nonionic and ionic surfactant solutions (Barber *et al.*, 1991; Kano *et al.*, 1991; Kile and Chiou, 1989). The dimerization of oleate in aqueous solutions resulted a decrease of slope in γ–log C curve at increasing concentration (γ = surface tension, C = surfactant concentration) (Somasundaran *et al.*, 1984). Some dye–surfactant aggregates were also reported in the premicellar region (Atherton and Dymond, 1989; Dakiky and Nemcova, 2000; Neumann and Gehlen, 1990; Yamagishi, 1982).

Dimerization of ionic amphiphiles in water has been reported according to some experimental observations (Franks and Smith, 1964; Oakenfull and Fisher, 1977; Somasundaran *et al.*, 1984) and theoretical modeling (Somasundaran *et al.*, 1984; Vold, 1987, 1990, 1992). Mukerjee (1958, 1965) and Mukerjee *et al.* (1958) measured the conductivity and osmotic coefficient and concluded that the amphipathic ions tend to form dimers. Vold (1992) proposed theoretically that (i) a critical micelle concentration exists where a small fraction of the material is present in a distribution of pre-micelles in equilibrium with the micelles and (ii) the amount in dimers is higher than in monomers, and thereafter decreases rapidly, becoming negligible above an aggregation number of four.

The aim of this work is to present new evidences for the existence of premicellar multimers below cmc by using a dynamic light scattering (DLS) system. Furthermore, it was observed that the multimers coexist with micelles in a narrow range of concentration near the cmc in the aqueous $C_{10}E_4$ solutions at 20 °C.

* Corresponding author. Tel.: +886 2 2737 6648; fax: +886 2 2737 6644.
E-mail address: sylin@mail.ntust.edu.tw (S.-Y. Lin).

0368-1653/$ – see front matter
doi:10.1016/j.jcice.2007.11.009

Nomenclature

C	bulk concentration of surfactant (mol/cm^3)
cmc	critical micelle concentration (mol/cm^3)
D	mutual translational diffusivity (cm^2/s)
D_h, D_{h1}, D_{h2}	hydrodynamic diffusivity (cm^2/s)
$G(\Gamma)$	the unknown line-width distribution function
$g^{(1)}(\tau)$	electric field correlation function
$g^{(2)}(\tau)$	the normalized intensity autocorrelation function
I	scattering light intensity of surfactant solution
I_{Bz}	scattering light intensity of liquid benzene
k_B	Boltzman's constant, 1.38×10^{-16} (erg/(mol K))
Mn	molecular weight (g/mol)
N, N_1, N_2	number of particle in solution
n_D^{20}	the refractive index of matching liquid at 20 °C
n_0	the refractive index of solvent
q	scattering vector (= $(4\pi n_0/\lambda_0)\sin(\theta/2)$)
R_g	radius of gyration
R_h	hydrodynamic radius
T	temperature (K)
T_c	the cloud point of surfactant solution

Greek symbols

β	A_{coh}/A, a non-ideality factor
γ	surface tension (mN/m)
Γ	relaxation rate or line-width
η	the viscosity of solvent
λ_0	wavelength of light
θ	scattering angle
τ	delay time

This paper first details the experimental methods, then the measured results, and ends with a conclusion and discussions section.

2. Experimental

2.1. Materials

Nonionic surfactant $C_{10}E_4$ (decyl tetraethylene glycol ether, $C_{10}H_{21}(OCH_2CH_2)_4OH$) purchased from Nikko, Japan; (purity >99%). Benzene (with purity >99%) is purchased from ACROS. Matching liquid (decalin, cis + trans; >98%; reflection index $n_D^{20} = 1.474$) is from Fluka. Poly(ethylene glycol) (PEG, molecular weight ranges from 225 to 22,500) are from Fluka and Aldrich. Surfactants and PEGs were used without further modification. Aqueous solutions were prepared with clean water purified via a Barnstead NANOpure water purification system, with the output water having a specific conductance of less than 0.057 $\mu\Omega^{-1}$/cm. All solutions were diluted from a mother solution to eliminate errors in sample preparation and were used without any filtration treatment. To prevent the contamination of dust, solution preparation was undertaken in a Laminar Flow with HEPA filters (Class 100, Tsao Hsin Co.). Sample preparation has been detailed in our previous work (Lee *et al.*, 2002).

2.2. Apparatus

Particles of aggregating clusters were measured by using a dynamic light scattering (DLS) system for aqueous $C_{10}E_4$ solutions at 20 °C. The DLS system was composed of a BI-200SM goniometer, a BI-9000AT digital correlator (522 channels, Brookhaven), a 2 W Ar laser light source (Lexel), a temperature probe with thermometer (stability ± 0.04 °C; 5622 and 1506, Hart Scientific) and a thermostatic circulator (with temperature stability ±0.01 °C; HD, Julabo). The temperature probe is inserted in the matching liquid about 5 mm from the sample tube. Sample solution is put in a glass tube with inside diameter of 10 mm. The temperature variation for the solution during the DLS measurement is less than 0.1 °C. Shown in Fig. 1 is a representative temperature relaxation during a measurement for 8 h.

Light of 514.5 nm wavelength was used and the scattered light at 90° was collected. The intensity (I) was calibrated against benzene (I_{Bz}). Parts of the samples were repeated by collecting the scattered light at 120° for confirmation. The scattered light intensity was fairly weak due to the extremely dilute $C_{10}E_4$ concentration. For solutions at $C \leq 0.92$ μmol/mL, the measurements were taken with a power of 700 mW and a 400 mm pinhole for several hours in order to get sufficient confidence. For example, the data were collected for 7 h for the solution of $C = 0.875$ μmol/mL. A longer time is needed for a more dilute solution.

2.3. DLS measurement

The measured $g^{(2)}(\tau)$, the normalized intensity autocorrelation function, is related to the electric field correlation function $g^{(1)}(\tau)$ by the Siegert relation (Chu, 1974; Siegert, 1943):

$$g^{(2)}(\tau) = 1 + \beta|g^{(1)}(\tau)|^2 \quad (1)$$

where β is a non-ideality factor accounting for the deviation from the ideal correlation and τ is the delay time. For a polydisperse sample with a continuous distribution of sizes, correlation function $g^{(1)}(\tau)$ can be represented by a superposition of exponential

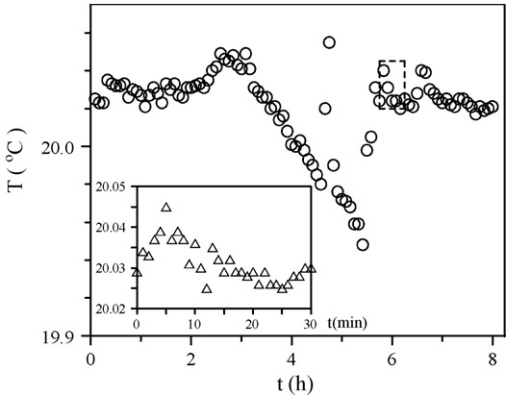

Fig. 1. Temperature variation of matching liquid (5 mm away from the sample tube) during the DLS measurement. The inset enlarges the temperature relaxation of the broken box.

decays (Schillén *et al.*, 1994):

$$|g^{(1)}(\tau)| = \int_0^\infty G(\Gamma)\exp(-\Gamma\tau)\,d\Gamma \quad (2)$$

where $G(\Gamma)$ represents the distribution of relaxation rates (Γ) and is resulted from the fit on $g^{(1)}(\tau)$. Under the condition of $qR_g < 1$ (R_g is the radius of gyration) (Zhou and Chu, 1988), the relaxation rate is related to the translational diffusivity (D) by $\Gamma = Dq^2$. Here, q is the scattering vector (=$(4\pi n_0/\lambda_0)\sin(\theta/2)$), n_0 is the refractive index of solvent, λ_0 is the wavelength of light, and θ is the scattering angle. The particles are assumed to be hard spheres in dilute solution and the Stokes–Einstein equation is used to relate the diffusivity D and hydrodynamic diameter D_h (=$2R_h$) (Bird *et al.*, 1960):

$$R_h = \frac{k_B T}{6\pi\eta D} \quad (3)$$

where k_B is the Boltzman constant, and η is the viscosity of solvent at temperature T. In this work, $g^{(1)}(\tau)$ was analyzed by the constrained regularized CONTIN program of ISDA software packet from Brookhaven (Provencher, 1982a,b). To verify the fitting results, the Exponential Sampling and Cumulant methods were also applied from time to time.

2.4. Lower size limit

The lower size limit of DLS system depends on the sample concentration, refractive index and the laser power. It is commonly accepted that to measure smaller sizes of particles, a more powerful laser is required, and a shorter wavelength can help considerably.

Aqueous PEG (different molecular weight as listed in Table 1) solutions were used for studying the lower size, or molecular weight, limit of our DLS system. PEG solutions of 0.1 or 0.2 wt% were first stirred at 50 °C for 1 h, then isolated at dark for 2 days to equilibrate and to avoid exposure to sunlight that might cause PEG degradation. They were occasionally gently stirred using a magnetic stirrer. Before the measurement, the aggregation particles were removed by ultra-centrifugal filtration (in general, 400 kg for 2 or 3 h; Beckman Coulter, Optima L-90 K; detailed in Table 1). The middle part of solutions in the centrifugal tube was then moved to the sample cell for the DLS measurement. The DLS measurement was performed at 20.0 ± 0.1 °C. The correlation function $g^{(1)}(\tau)$ was analyzed by the CONTIN program.

2.5. Surface tension

The cmc evaluated from the surface tension (γ) method for $C_{10}E_4$ solutions was obtained by using a video-enhanced pendant bubble tensiometer (Lin *et al.*, 1990; Lin and Hwang, 1994). The tensiometer creates a silhouette of a pendant bubble, video-images the silhouette, and digitizes the image. The pendant bubble was generated in a $C_{10}E_4$ aqueous solution, which was put inside a quartz cell. The quartz cell was enclosed in a thermostatic air chamber, and the temperature variation of the surfactant solutions is less than ±0.05 °C. A 17-gauge stainless steel inverted needle (1.07 mm i.d.; 1.47 mm o.d.), which was connected to the normally closed port of a three-way miniature solenoid valve, was used for the bubble generation. Parallel light with constant intensity passes through the pendant bubble and forms a silhouette of the bubble on a solid-state video camera. The silhouette image was digitized into 480 lines × 512 pixels with a level of gray with 8-bit resolution. The edge is defined as the position with an intensity of 127.5. The edge coordinates of the pendant bubble were fitted with the classical Laplace equation to find the surface tension. The accuracy and reproducibility of γ obtained by this technique are ca. 0.1 mN/m (Lin *et al.*, 1995, 1996). Surface tension γ decreases at increasing $C_{10}E_4$ concentration (C) and reaches a constant value as the surface concentration becomes saturated. The cmc of surfactant solution is determined from the break point of the γ–log C data profile.

2.6. Cloud point

The surfactant solutions are prepared in flasks and placed in a water thermostat with temperature stability ±0.1 K for several days to allow the system to reach equilibrium. During the equilibration process, the samples are stirred at 200 rpm several times to ensure through mixing. After equilibrium is reached, the samples are moved to the sample tubes for the DLS measurement. The cloud point is determined from the turning point of the I/I_{Bz} vs. temperature curve (see later in the inset of Fig. 4).

Table 1
Physical properties of poly(ethylene glycol)

PEG	Company[a]	Mw	Mn	PDI	C (wt%)	Centrifugal filtration (kg)	Filtration time (h)	D_h (nm)
20K	F	22,500	21,200	1.06	0.1	170	3	9.3
10K	A		10,000		0.1	400	3	5.6
8K	F	8,350	8,100	1.03	0.1			4.5
4.6K	A		4,600		0.2	400	2	4.1
2K	A		2,000		0.1	400	3	2.2
1K	A		1,000		0.2	400	2	1.5
600	A		600		0.2	400	2	1.3
550	F	580	550	1.05	0.1	170	3	1.2
400	A		400		0.2	400	2	
200	A	225.4	200	1.13	0.2	400	2	

[a] F: Fluka, A: Aldrich.

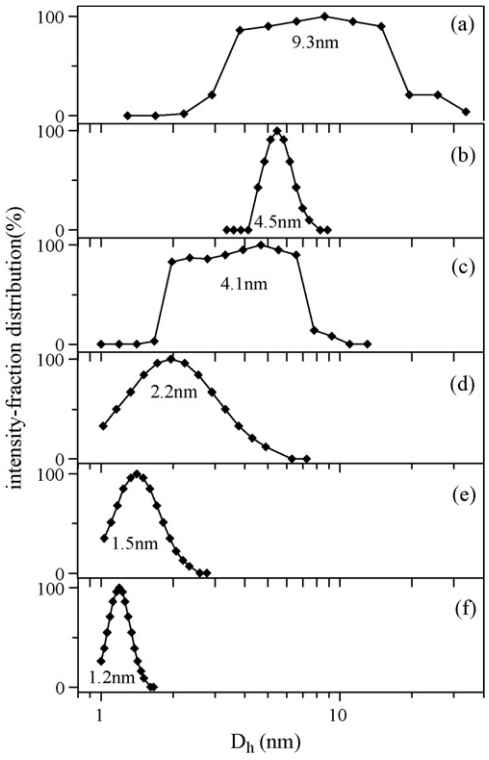

Fig. 2. Intensity-fraction distribution for PEG solutions obtained from the CONTIN model: Mn = (a) 21,200, (b) 10,000, (c) 4600, (d) 2000, (e) 1000, and (f) 550 g/mol.

3. Results

3.1. PEG

The intensity-fraction distribution of PEG of different molecular weight is shown in Fig. 2. The correlation functions for PEG solutions of Mn = 200 and 400 are very close to that of pure water. Therefore, the lower molecular weight limit for PEG of our DLS system is around Mn = 550 and an average D_h of 1.2 is resulted. Note that the intensity-fraction distribution for PEG of Mn = 550 is not complete. The true average D_h will be a little bit smaller than 1.2 nm.

For the molecular weight range 1000–22,500, a log–log plot of the hydrodynamic radius (R_h) against molecular weight (Mn) is presented in Fig. 3. The following relation was established by using a direct power law fit of R_h to Mn:

$$R_h = 0.0134\,\mathrm{Mn}^{0.58}\,\mathrm{nm} \quad (4)$$

The exponent 0.58 is in good agreement both with asymptotic values from the Flory prediction (Flory, 1953) of 0.6 and with the renormalization group calculation value of 0.588 (Devanand and Selser, 1991; Le Guillou and Zinn-Justin, 1977; Weill and Descloizeaux, 1979). It is therefore concluded that PEG in water at 20 °C exhibits asymptotic good solvent behavior. Note that the measured R_h for Mn = 600 and 550 deviates, showing a larger radius, from the straight line.

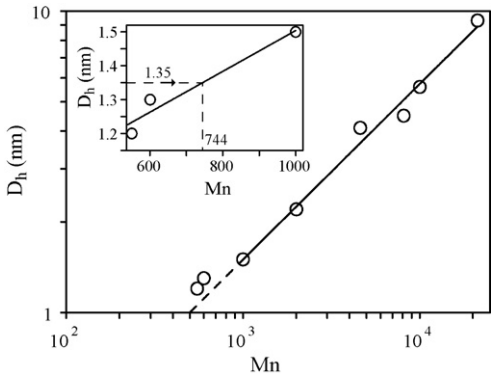

Fig. 3. Log–log plot of the PEG hydrodynamic radius versus molecular weight.

3.2. Cloud point

The cloud point (T_c) of aqueous $C_{10}E_4$ solution decreases at increasing concentration as shown in Fig. 4. The working concentration in this study is less than 3 μmol/mL. T_c is larger than 21 °C at $C < 3$ μmol/mL, therefore all $C_{10}E_4$ solutions in this work are below their T_c.

3.3. cmc

The cmc of aqueous $C_{10}E_4$ solution is determined from the break point (Fig. 5(a)) of the γ–log C data profile and cmc = 0.77 μmol/mL from the surface tension data. The cmc from the scattered light intensity is commonly determined from the turning point of the I/I_{Bz} vs. C curve. The scattered intensities of aqueous $C_{10}E_4$ solutions are shown in Fig. 5(b). The value of I/I_{Bz} deviates the base line of the dilute solutions and increases significantly as $C \geq 0.84$ μmol/mL (the diamonds in Fig. 5(b)). This indicates that large aggregating clusters or micelles begin to form in surfactant solutions at $C \geq 0.84$ μmol/mL. Therefore, cmc = 0.84 μmol/mL from the DLS intensity data.

3.4. Autocorrelation function

The change of I/I_{Bz} at $C <$ cmc (0.84 μmol/mL) is insignificant in Fig. 5(b) (see points A and B for $C = 0.72$

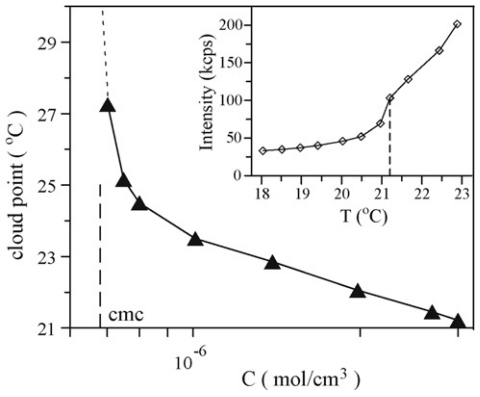

Fig. 4. The cloud point as a function of bulk concentration of $C_{10}E_4$. The inset shows the variation of scattered light intensity as a function of temperature at $C = 3.0$ μmol/mL.

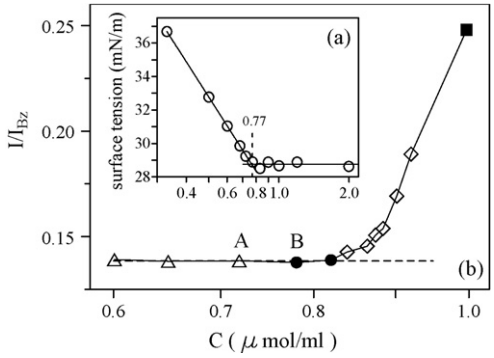

Fig. 5. (a) Equilibrium surface tension of $C_{10}E_4$ solutions at $T = 20 \pm 0.1$ °C. (b) Dimensionless scattered light intensity (I/I_{Bz}) as a function of $C_{10}E_4$ concentration at 20 ± 0.05 °C.

and 0.78 μmol/mL). However, there is a large difference in the normalized time autocorrelation functions for solutions of these concentrations. Fig. 6 shows that the correlation function for solutions of $C \leq 0.72$ μmol/mL (for example, 0.65 μmol/mL, curve 1) is nearly indistinguishable from that for pure water (dashed curve). Nevertheless, the correlation functions for solutions of $C \geq 0.78$ μmol/mL (curve 2) depart clearly from pure water. As the concentration increases, the correlation function departs from pure water more significantly (curves 3–6 in Fig. 6).

The normalized time autocorrelation functions of $C_{10}E_4$ solutions are fitted with either the CONTIN or Exponential Sampling (ExpSam) models. The fits are excellent and nearly same particle distributions result from both models. Fig. 7 shows three representative examples for the fits from both models for 0.78, 0.92 and 0.997 μmol/mL.

Small aggregating clusters with diameter around 1.1 nm were detected for solutions of 0.78 and 0.82 μmol/mL. Fig. 8(a and b) show the particle distributions. Note that the scattered light (I/I_{Bz}, in Fig. 5(b)) for these two solutions is nearly the same as the solutions without clusters ($C = 0.60$ and 0.65 μmol/mL). However, the correlation functions do increase significantly and particles of 1.0 and 1.2 nm result from the CONTIN model for

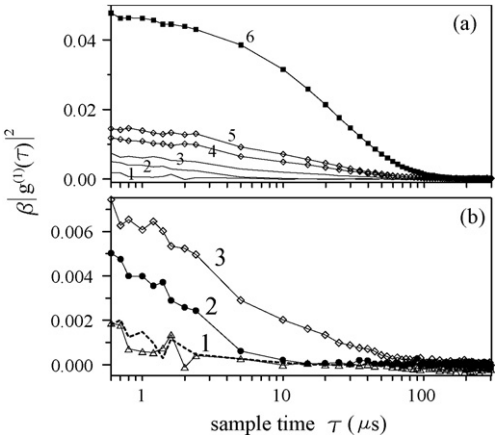

Fig. 6. Normalized time autocorrelation function of scattered intensity for different $C_{10}E_4$ concentrations: (1) 0.649, (2) 0.781, (3) 0.875, (4) 0.902, (5) 0.920, (6) 0.997 μmol/mL. The dashed curve in (b) is the correlation function of pure water.

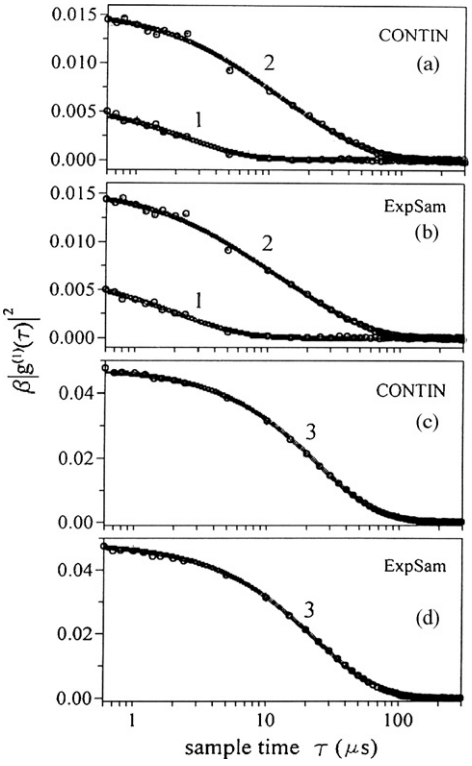

Fig. 7. The normalized time autocorrelation functions of $C_{10}E_4$ solutions fitted by the CONTIN (a and c) and Exponential Sampling (b and d) models for solutions at C = (1) 0.781, (2) 0.920, and (3) 0.997 μmol/mL.

these two solutions, respectively. It is believed that these aggregating clusters are the premicellar multimers.

At higher concentrations, I/I_{Bz} increases significantly (the diamonds in Fig. 5(b)) and the other group of larger particles around 10 nm is detected in solutions (Fig. 8). We believe the larger particles are the micelles of $C_{10}E_4$ at concentrations around 0.85–1.0 μmol/mL.

Two separated groups of aggregating clusters result from the CONTIN model for solutions of 0.84–0.92 μmol/mL (Fig. 8). The smaller clusters have an average diameter (D_h) of 1.35 nm and $D_h = 10.5$ nm for the larger ones. Therefore, there coexist aggregating multimers (1.35 nm) and micelles (10.5 nm) of $C_{10}E_4$. These $C_{10}E_4$ multimers should be called "submicellar" multimers instead of premicellar multimers since they, submicellar multimers and micelles, coexist in solution.

At higher concentrations ($C \geq 0.997$ μmol/mL), only the micelles are detected in solutions. It is probably that the scattered light of the micelles becomes stronger and stronger at increasing concentration and therefore the signal from the submicelles becomes too weak to be detected. This trend can also be observed from the intensity-fraction distribution shown in Fig. 8. The peaks of scattered light for micelles and submicelles grow and decline, respectively, at increasing $C_{10}E_4$ concentration. This indicates that the amount of micelles increases with $C_{10}E_4$ concentration and therefore the intensity of scattered light contributed from micelles dominates at $C \geq 0.997$ μmol/mL.

Note that nearly same particle distributions were observed from the Exponential Sampling model. Fig. 9 shows three

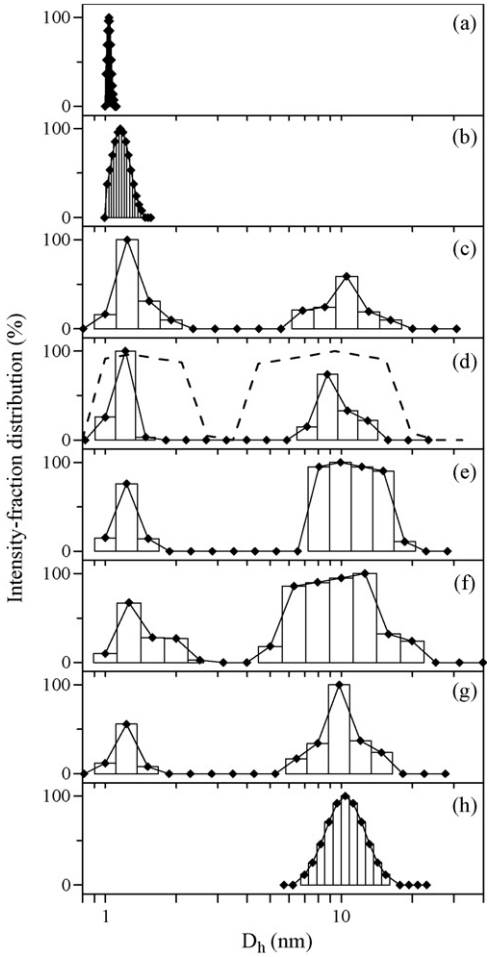

Fig. 8. Intensity-fraction distribution for $C_{10}E_4$ solutions obtained from the CONTIN model at concentrations around cmc: C = (a) 0.781 (duration = 8 h), (b) 0.820 (12 h), (c) 0.864 (12 h), (d) 0.875 (2 h (the dashed one) and 8 h (the solid one)), (e) 0.884 (8 h), (f) 0.902 (2 h), (g) 0.920 (4 h), and (h) 0.997 (1 h) μmol/mL.

examples for C = 0.82, 0.86, and 0.92 μmol/mL. The averaged hydrodynamic diameters (D_h) of the pre-micelles, sub-micelles, and micelles of $C_{10}E_4$ at different bulk concentrations are shown in Fig. 10.

The intensity-fraction distribution (Fig. 8) depends upon the duration of the measurement. Usually, a sharper size distribution results from a longer duration. For example, Fig. 8(d) shows the data acquired for 2 h (the dashed curve) and 8 h (the solid curve) for C = 0.875 μmol/mL; a broad peak shown in Fig. 8(f) was resulted from a shorter duration (2 h). The durations for the runs in Fig. 8 are detailed in the figure caption.

Some measurements are repeated with the angle being changed to 120°, at which the scattered data are collected. The correlation functions obtained at 120° yields a similar result.

The size of micelles of $C_{10}E_4$ depends upon the bulk concentration (C) and temperature (T). Fig. 11 illustrates the dependence on C and T. Smaller micelles were observed at a lower T for $C_{10}E_4$. As C increases, larger $C_{10}E_4$ micelles result. For example, D_h of micelles grows up from 10.5 to 28.4 nm as C increases from 1.0 to 3.0 μmol/mL at T = 20 °C. Smaller

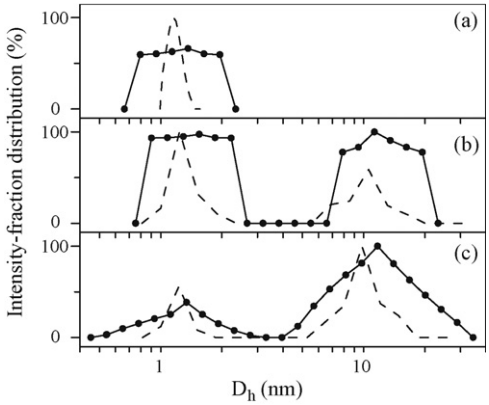

Fig. 9. Comparison on the intensity-fraction distribution obtained from the CONTIN (dashed curves) and Exponential Sampling (solid curves) models for C = (a) 0.820, (b) 0.864, and (c) 0.920 μmol/mL.

micelles (D_h = 24.1 nm) were obtained for C = 3 μmol/mL at T = 18 °C. The size of the $C_{10}E_4$ micelles is similar to that of $C_{12}E_5$ and $C_{12}E_6$ at 20 °C (Brown and Rymdén, 1987; Feitosa *et al.*, 1996), $C_{12}E_8$ at 25 °C (Kamenka *et al.*, 1991), and $C_{12}E_{20}$ at 30 °C (Abe *et al.*, 1992). Parts of the literature data are also shown in Fig. 11.

According to the I/I_{Bz} data from DLS, cmc is around 0.84 μmol/mL. The correlation function tells that this is the concentration for micelles starting to appear in solution. In other words, the change of intensity of the scattered light at the formation of pre-micelles is insignificant (Fig. 5(b)), and therefore, it is not detectable for aqueous $C_{10}E_4$ solutions. This is because the diameter of $C_{10}E_4$ pre-micelles is pretty small, only around 1.1 nm at this concentration. Nevertheless, the surface tension data predict cmc = 0.77 μmol/mL and do reflect the property changes in solution and in air–water interface as the pre-micelles appear.

At C = 0.78 μmol/mL, the pre-micelles of $C_{10}E_4$ start to appear in the bulk phase and the amount of pre-micelles increases with bulk concentration. As the concentration is around but less than 0.84 μmol/mL (right before the formation of micelles), it is believed there are a huge amount of pre-micelles in solution. A rough mass balance calculation was performed here. At C = 0.84 μmol/mL, around 3.6×10^{19} and 4.7×10^{20} molecules of $C_{10}E_4$ are in the states of sub-micelles and monomers, respectively, in 1 L of solution. In other words,

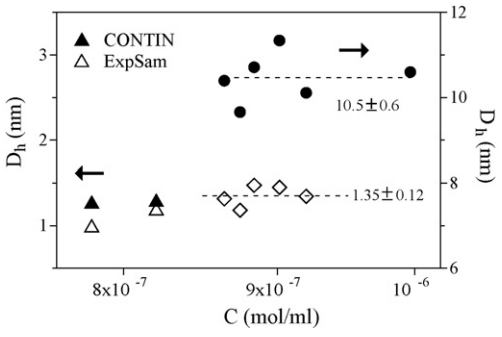

Fig. 10. Hydrodynamic diameter (D_h) of $C_{10}E_4$ micelles (●), sub-micelles (◇), and pre-micelles (△ and ▲) as a function of bulk concentration at 20 °C.

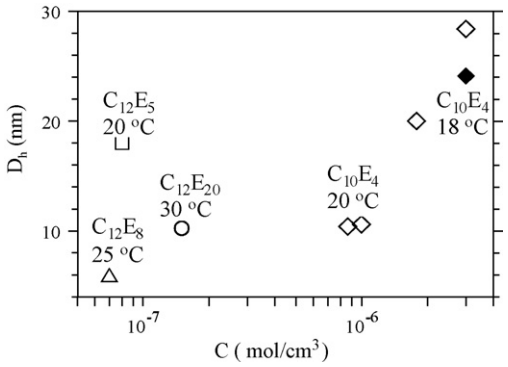

Fig. 11. Hydrodynamic diameter (D_h) of C_mE_n micelles as a function of bulk concentration and temperature. T = 18 °C (◆) and 20 °C (◇).

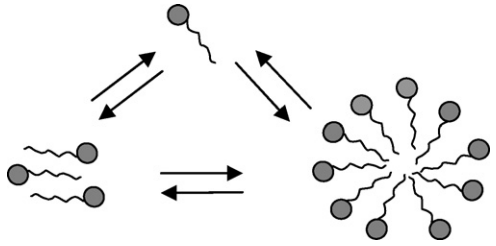

Fig. 12. A cartoon describing the exchange of surfactant molecules between the micelles, sub-micelles, and water phase.

there are about 10^{19} pre-micelles/L of solution, by assuming that a few $C_{10}E_4$ molecules aggregate and form a pre-micelle.

At C = 0.84 μmol/mL, micelles start to appear in $C_{10}E_4$ solution. In the intensity–fraction distribution diagram the peak of micelles should be much weaker than the peak of sub-micelles since the amount of micelles is much less than the sub-micelles. Note that the scattered light (I) depends upon the number (N) and the size (D_h) of particles with a relationship: $I \propto ND_h^6$. The peaks for the micelles and sub-micelles should grow and decline, respectively, as C increases (Fig. 8). These two peaks will show roughly equal intensity when there are about 10^{14} micelles/L of solution (i.e., $N_1D_{h1}^6 = N_2D_{h2}^6$). As the $C_{10}E_4$ concentration further increases, the number of micelles increases and the peak of micelles will become stronger and stronger, therefore, the peak of sub-micelles may become too weak to be detected.

A cartoon illustrating the coexistence of monomers, sub-micelles, and micelles at C = 0.84–0.92 μmol/mL and the exchange of surfactant molecules between them is shown in Fig. 12.

4. Conclusion and discussions

The formation of pre-micelles, sub-micelles, and micelles of $C_{10}E_4$ in aqueous solution were studied. The scattered light intensity and normalized time autocorrelation functions from a dynamic light scattering system reveal the existence of pre-micelles and the coexistence of sub-micelles and micelles. This is exactly the same as what Vold (1992) proposed from theoretical simulations.

It is illustrated from the DLS data that for $C_{10}E_4$ aqueous solutions: (1) at $C \leq 0.72$ μmol/mL, the correlation function is indistinguishable from that for pure water; (2) at C = 0.78–0.82 μmol/mL monomers and premicellar multimers coexist; (3) at C = 0.84–0.92 μmol/mL, monomer + submicellar multimers + micelles coexist; and (4) at more elevated concentrations, only the signals from the micelles are detected.

The $C_{10}E_4$ concentration is pretty dilute for the solutions showing the coexistence of sub-micelles and micelles. Therefore, the DLS measurement must be performed with a strong power (700 mW in this work) and a large pinhole opening (400 mm) for several hours. The success of this measurement relies on (i) the thorough cleaning of sample cells, (ii) the purity of water and surfactant, (iii) how to prevent aqueous solutions from the dust in air, and (iv) an excellent stability of laser light. A laminar flow with HEPA filters (class 100) was applied for the solution preparation. A power stabilizer (with less than ±1% output) was installed for the laser. Fig. 13 shows a representative stability of count rate for C = 0.92 μmol/mL for 6 h, which shows a nearly excellent stability.

To estimate the aggregation number of the submicellar multimers, a rough but simple calculation was performed. It is presumed that the particle is spherical and formed by $C_{10}E_4$ only. The bulk density of the multimers is assumed to be the same as liquid $C_{10}E_4$, 0.955 g/mL. A sphere with 1.35 nm diameter contains about 2.2 $C_{10}E_4$ molecules. Fig. 8 shows that the particle distribution for the sub-micelles ranges roughly from 1.0 to 2.0 nm. A sphere consisting of 1–6 $C_{10}E_4$ molecules has a diameter of 1.03, 1.31, 1.49, 1.64, 1.77 and 1.88 nm, respectively, according to above estimation. Therefore, it is proposed from this rough calculation that dimers are the major component of sub-micelles. This particle distribution for the submicellar multimers is similar to what Vold (1992) proposed from theoretical modeling: the amount in dimers is higher than in monomers, and thereafter decreases rapidly, becoming negligible above an aggregation number of 4.

The data from the above estimation was also confirmed in the inset of Fig. 3. An aggregation particle with D_h = 1.35 corresponded to a PEG of molecular weight 744 g/mol from the presumed linear relation between the data of 550–1000 g/mol of Mn. $C_{10}E_4$ has Mw of 334.5 g/mol, and an average molecular weight of 744 g/mol implies an aggregating cluster with 2.2 $C_{10}E_4$ molecules.

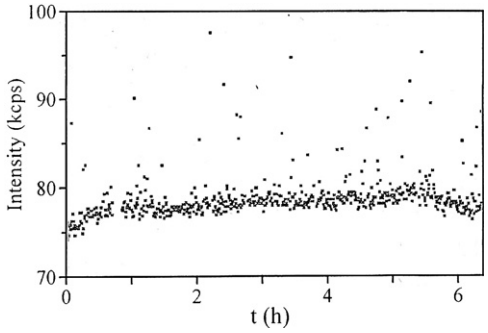

Fig. 13. Variation of the scattered light intensity during the measurement for 0.92 μmol/mL.

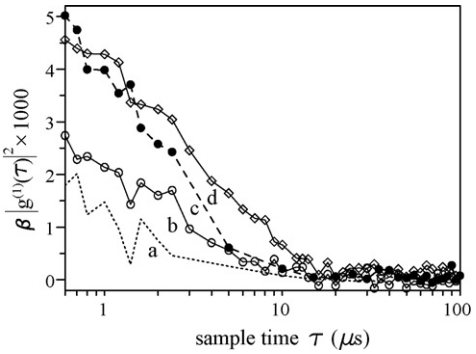

Fig. 14. Normalized time autocorrelation function of scattered intensity for (a) pure water, (b) PEG solution with Mn = 550 g/mol, (c) $C_{10}E_4$ solution with $C = 0.781$ μmol/mL, and (d) PEG solution with Mn = 1000 g/mol.

Fig. 14 shows the normalized time autocorrelation function of scattered intensity for pure water (dotted curve, a), PEG solutions with Mn = 550 and 1000 (curves b and d, respectively), and $C_{10}E_4$ solution with $C = 0.781$ μmol/mL (dashed curve, c). If the scattered intensities resulted from PEG molecules and $C_{10}E_4$ multimer clusters are the same, the autocorrelation functions in Fig. 14 indicate that the pre-micelles should have a molecular weight ranging between 550 and 1000 g/mol.

Recently, the coexistence of submicellar multimers and micelles at concentrations near the cmc has also been observed for other nonionic surfactants $C_{10}E_8$ and Triton-X 100 in our lab.

Acknowledgements

We are indebted to L.J. Chen and H.K. Tsao for many helpful discussions. This work is supported by the National Science Council of Taiwan (grant NSC 90-2214-E-011-024).

References

Abe, M., H. Uchiyama, T. Yamaguchi, T. Suzuki, and K. Ogino, "Micelle Formation by Pure Nonionic Surfactants and Their Mixtures," *Langmuir*, **8**, 2147 (1992).

Atherton, S. J. and C. M. G. Dymond, "Formation of Clusters between Ionic Species and Sodium Dodecyl Sulfate below the Critical Micelle Concentration. Ethidium Ions and Divalent Metal Ions," *J. Phys. Chem.*, **93**, 6809 (1989).

Barber, D. C., R. A. Freitag-Beeston, and D. G. Whitten, "Atroplsomer-Specific Formation of Premicellar Porphyrin J-Aggregates in Aqueous Surfactant Solutions," *J. Phys. Chem.*, **95**, 4074 (1991).

Bird, R. B., W. E. Stewart, and E. N. Lightfoot, *Transport Phenomena*, p. 514, John-Wiley and Sons, Inc, New York, U.S.A. (1960).

Brown, W. and R. Rymdén, "Static and Dynamical Properties of a Nonionic Surfactant ($C_{12}E_6$) in Aqueous Solution," *J. Phys. Chem.*, **91**, 3565 (1987).

Bruhn, H. and J. Holzwarth, "Electron-Transfer Reactions between Transition-Metal Complexes in Micellar Solutions," *Ber. Bunsen-Ges. Phys. Chem.*, **82**, 1006 (1978).

Cho, J. R. and H. Morawetz, "Catalysis of Ionic Reactions by Micelles. Reaction of $Co(NH_3)_5C1^{2+}$ with Hg^{2+} in Sodium Alkyl Sulfate Solutions," *J. Am. Chem. Soc.*, **94**, 375 (1972).

Chu, B., *Laser Light Scattering: Basic Principles and Practice*, 2nd Ed., Chapter 3, Academic Press, Boston, U.S.A. (1974).

Dakiky, M. and I. Nemcova, "Aggregation of *o,o'*-Dihydroxy azo Dyes III. Effect of Cationic, Anionic and Non-ionic Surfactants on the Electronic Spectra of 2-Hydroxy-5-Nitrophenylazo-4-[3-Methyl-1-(4-Sulfophenyl)-5-Pyrazolone]," *Dyes Pigm.*, **44**, 181 (2000).

Devanand, K. and J. C. Selser, "Asymptotic Behavior and Long-Range Interactions in Aqueous Solutions of Poly(ethylene oxide)," *Macromolecules*, **24**, 5943 (1991).

Feitosa, E., W. Brown, M. Vasilescu, and M. Swanson-Vethamuthu, "Effect of Temperature on the Interaction between the Nonionic Surfactant $C_{12}E_5$ and Poly(ethylene oxide) Investigated by Dynamic Light Scattering and Fluorescence Methods," *Macromolecules*, **29**, 6837 (1996).

Flory, P. J., *Principles of Polymer Chemistry*, Chapter 14, Cornell University press, Ithaca, New York, U.S.A. (1953).

Franks, F. and H. T. Smith, "The Association and Hydration of Sodium Dodecyl Sulfate in the Submicellar Concentration Range," *J. Phys. Chem.*, **68**, 3581 (1964).

Holzwarth, J., W. Knoche, and B. H. Robinson, "Catalysis of Metal-Complex Formation on Micelle Surfaces—Reaction between Divalent Metal-Ions and Pada in Presence of Sodium Dodecyl-Sulfate," *Ber. Bunsen-Ges. Phys. Chem.*, **82**, 1001 (1978).

Kamenka, N., M. E. Amrani, J. Appell, and M. Lindheimer, "Mixed Micelle-to-Vesicle Transition in Aqueous Nonionic Phospholipid Systems," *J. Colloid Interface Sci.*, **143**, 463 (1991).

Kano, K., S. Tatemoto, and S. Hashimoto, "Specific Interactions between Sodium Deoxycholate and Its Water-Insoluble Analogues. Mechanisms for Premicelle and Micelle Formation of Sodium Deoxycholate," *J. Phys. Chem.*, **95**, 966 (1991).

Kile, D. E. and C. T. Chiou, "Water Solubility Enhancements of DDT and Trichlorobenzene by Some Surfactants below and above the Critical Micelle Concentration," *Environ. Sci. Technol.*, **23**, 832 (1989).

Lee, Y. C., Y. Y. Wang, M. W. Tang, H. S. Liu, and S. Y. Lin, "Effects of Temperature and Concentration on the Micellization of Nonionic Polyethoxylated Surfactants," *J. Chin. Inst. Chem. Engrs.*, **33**, 439 (2002).

Le Guillou, J. C. and J. Zinn-Justin, "Critical Exponents for the *n*-Vector Model in Three Dimensions from Field Theory," *Phys. Rev. Lett.*, **39**, 95 (1977).

Lin, S. Y., K. McKeigue, and C. Maldarelli, "Diffusion-Controlled Surfactant Adsorption Studied by Pendant Drop Digitization," *AIChE J.*, **36**, 1785 (1990).

Lin, S. Y. and H. F. Hwang, "Measurement of Low Interfacial Tension by Pendant Drop Digitization," *Langmuir*, **10**, 4703 (1994).

Lin, S. Y., L. J. Chen, J. W. Xyu, and W. J. Wang, "An Examination on the Accuracy of Interfacial Tension Measurement from Pendant Drop Profiles," *Langmuir*, **11**, 4159 (1995).

Lin, S. Y., W. J. Wang, L. W. Lin, and L. J. Chen, "Systematic Effects of Bubble Volume on the Surface Tension Measured by Pendant Bubble Profiles," *Colloids Surf. A*, **114**, 31 (1996).

Mukerjee, P., "Dilute Solutions of Amphipathic Ions. IV. Some General Effects of Dimerization," *J. Phys. Chem.*, **62**, 1404 (1958).

Mukerjee, P., "Dimerization of Anions of Long-Chain Fatty Acids in Aqueous Solutions and the Hydrophobic Properties of the Acids," *J. Phys. Chem.*, **69**, 2821 (1965).

Mukerjee, P., K. J. Mysels, and C. I. Dulin, "Dilute Solutions of Amphipathic Ions. I. Conductivity of Strong Salts and Dimerization," *J. Phys. Chem.*, **62**, 1390 (1958).

Neumann, M. G. and M. H. Gehlen, "The Interaction of Cationic Dyes with Anionic Surfactants in the Premicellar Region," *J. Colloid Interface Sci.*, **135**, 209 (1990).

Oakenfull, D. G. and L. R. Fisher, "The Role of Hydrogen Bonding in the Formation of Bile Salt Micelles," *J. Phys. Chem.*, **81**, 1838 (1977).

Pérez-Benito, E. and E. Rodenas, "Acid Hydrolysis of Reduced form of Nicotin–Adenin Dinucleotide in Sodium Dodecyl Sulfate Micelles," *J. Colloid Interface Sci.*, **139**, 87 (1990).

Provencher, S. W., "A Constrained Regularization Method for Inverting Data Represented by Linear Algebraic or Integral Equations," *Comput. Phys. Commun.*, **27**, 213 (1982a).

Provencher, S. W., "CONTIN: A General Purpose Constrained Regularization Program for Inverting Noisy Linear Algebraic and Integral Equations," *Comput. Phys. Commun.*, **27**, 229 (1982b).

Schillén, K., W. Brown, and R. M. Johnsen, "Micellar Sphere-to-Rod Transition in an Aqueous Triblock Copolymer System. A Dynamic Light Scatter-

ing Study of Translational and Rotational Diffusion,'' *Macromolecules*, **27**, 4825 (1994).

Siegert, A. J. F., MIT Radiation Lab., Report No. 465 (1943).

Somasundaran, P., K. P. Ananthapadmanabhan, and I. B. Ivanov, ''Dimerization of Oleate in Aqueous Solutions,'' *J. Colloid Interface Sci.*, **99**, 128 (1984).

Uppu, R. M., ''Phenazine/Dihydrophenazine Redox Couple as an Inoffensive Catalytic Probe Discerns Premicellar Aggregation in Dilute Aqueous Solutions of Triton X-100,'' *Langmuir*, **11**, 1038 (1995).

Vold, M. J., ''Premicelles: Hydrophobic Effect for the Dimer of Sodium *n*-Dodecyl Sulfate,'' *J. Colloid Interface Sci.*, **116**, 129 (1987).

Vold, M. J., ''Micellization: Some Properties of Dimers of Sodium *n*-Octyl and *n*-Dodecyl Sulfates,'' *J. Colloid Interface Sci.*, **135**, 520 (1990).

Vold, M. J., ''Micellization Process with Emphasis on Premicelles,'' *Langmuir*, **8**, 1082 (1992).

Weill, G. and J. Descloizeaux, ''Dynamics of Polymers in Dilute-Solutions—Explanation of Anomalous Indexes by Crossover Effects,'' *J. Phys.*, **40**, 99 (1979).

Yamagishi, A., ''Specific Interactions between Dye Cations in Premicellar Aggregates as Revealed by Electric Dichroism Measurements,'' *J. Colloid Interface Sci.*, **86**, 468 (1982).

Zhou, Z. and B. Chu, ''Anomalous Micellization Behavior and Composition Heterogeneity of a Triblock ABA Copolymer of (A) Ethylene Oxide and (B) Propylene Oxide in Aqueous Solution,'' *Macromolecules*, **21**, 2548 (1988).